

## Gold Catalysis | Hot Paper |

Javier Miró,<sup>[a]</sup> María Sánchez-Roselló,<sup>[a, b]</sup> Javier González,<sup>[c]</sup> Carlos del Pozo,<sup>\*[a]</sup> and Santos Fustero<sup>\*[a, b]</sup>

**Abstract:** A tandem gold-catalyzed hydroamination/formal aza-Diels–Alder reaction is described. This process, which employs quaternary homopropargyl amino ester substrates, leads to the formation of an intricate tetracyclic framework and involves the generation of four bonds and five stereocenters in a highly diastereoselective manner. Theoretical calculations have allowed us to propose a suitable mecha-

nistic rationalization for the tandem protocol. Additionally, by studying the influence of the ligands on the rate of the gold-catalyzed reactions, it was possible to establish optimum conditions in which to perform the process with a variety of substituents on the amino ester substrates. Notably, the asymmetric version of the tandem reaction was also evaluated.

## Introduction

The hydroamination reaction is a pivotal transformation in organic chemistry. It enables the direct formation of a new C–N bond by the addition of a nucleophilic nitrogen source to an unsaturated C–C bond in an atom-economical manner, from readily available alkenes and alkynes substrates.<sup>[1]</sup> The intramolecular version of this process gives direct access to nitrogen-containing heterocycles, which are present as recurrent scaffolds in naturally occurring molecules and biologically active compounds.<sup>[2]</sup> Despite its simplicity, this reaction suffers from a high activation barrier due to electrostatic repulsions between the electron density of the multiple bond and the nitrogen lone pair. One of the most common approaches to overcome this activation energy is the use of catalytic methods based on transition metal complexes.

In this context, the hydroamination of alkynes is especially important. They are more prone to undergo this type of transformation than their olefinic counterparts, and the in situ generated imines/enamines are suitable substrates for further cas-

cade transformations, which enables the formation of complex molecules in a one-pot fashion.

In the last decade, the development of gold catalysis has witnessed extraordinary growth. The unique features of gold salts, including exceptional alkynophilicity and low oxophilicity, make gold complexes well suited catalysts for the activation of alkenes, alkynes, and allenes. Hence, the activation of alkynes by gold salts provides a useful method for facilitating the addition of nitrogen nucleophiles, both inter- and intramolecularly, with high efficiency and under mild conditions.<sup>[3]</sup> Likewise, gold salts have shown exceptional properties for promoting tandem reactions, and there are numerous examples in the literature that combine a hydroamination step with further transformations.<sup>[4]</sup>

It is accepted that gold-catalyzed reactions of alkynes start with the electronic activation of the alkyne to generate a vinyl gold intermediate.<sup>[5]</sup> After evolution of this gold species, the last step of the reaction is protodeauration, which releases the product and regenerates the active catalytic species.<sup>[6]</sup> A recent study demonstrated how the nature of the ligands influences each stage of the catalytic cycle.<sup>[7]</sup> Actually, it is well known that ligands play a major role in tuning the reactivity and selectivity of gold complexes. The nature of the ancillary ligand directly influences the properties of the chemical bond between the gold and an unsaturated substrate. Therefore, the correct choice of ligand is crucial for the success of a gold-catalyzed transformation.<sup>[8]</sup>

Homopropargyl amines are common substrates in gold-catalyzed reactions. A wide variety of transformations have been devised that employ these substrates, which give access to several nitrogen-containing heterocycles.<sup>[9]</sup> However, to date, substrates bearing a quaternary stereocenter have not yet been tested. In the context of an ongoing project in our labo-

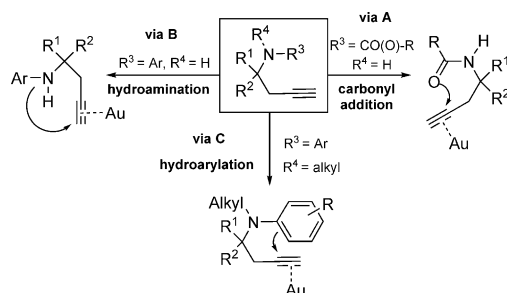
[a] J. Miró, Dr. M. Sánchez-Roselló, Dr. C. del Pozo, Prof. S. Fustero  
Departamento de Química Orgánica, Universidad de Valencia  
46100 Burjassot (Spain)  
E-mail: carlos.pozo@uv.es  
santos.fustero@uv.es

[b] Dr. M. Sánchez-Roselló, Prof. S. Fustero  
Laboratorio de Moléculas Orgánicas  
Centro de Investigación Príncipe Felipe  
46012 Valencia (Spain)

[c] Dr. J. González  
Departamento de Química Orgánica e Inorgánica  
Universidad de Oviedo, 33006 Oviedo (Spain)

 Supporting information for this article is available on the WWW under <http://dx.doi.org/10.1002/chem.201406224>.

ratory, we evaluated the reactivity of protected quaternary homopropargylic amino esters under gold catalysis. We anticipated that, depending on the nature of the N-protecting group, we could expect differential reactivity with these substrates. Accordingly, when the amino ester substrates contain a carbamate or an amide functionality, we would expect a nucleophilic carbonyl addition across the triple bond to occur (Scheme 1, **via A**).<sup>[10]</sup> However, when they contain an aryl sub-

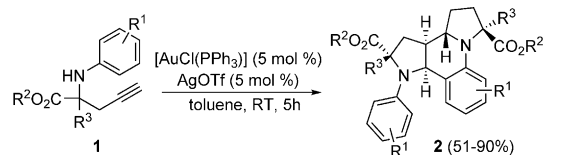


**Scheme 1.** Differential reactivity of quaternary homopropargyl amines under Au<sup>I</sup> catalysis.

stituent, they would react in the presence of gold salts through a hydroamination protocol (**via B**).<sup>[11]</sup> Finally, with substrates that bear a tertiary nitrogen group, the hydroamination reaction is blocked and a hydroarylation-type reactivity would be expected (**via C**).<sup>[12]</sup>

In fact, preliminary evaluation of the reactivity of homopropargyl amino esters **1** showed that substrates that bear an amide functionality (Scheme 1, R<sup>3</sup> = CO(O)-R) underwent a tandem carbonyl addition/nucleophilic addition/Petasis–Ferrer rearrangement in the presence of gold(I) salts to give 2,3-dihydropyridin-4-(1H)-ones in an efficient manner.<sup>[13]</sup> On the other hand, substrates that contain aromatic groups (R<sup>3</sup> = aryl) followed a tandem hydroamination/formal aza-Diels–Alder reaction sequence, which generated tetracyclic frameworks **2** in a single step (Scheme 2).<sup>[14]</sup> In the overall process, the simultaneous generation of four bonds and five stereocenters oc-

**Abstract in Spanish:** *En el presente trabajo se describe una reacción tándem hidroaminación/aza-Diels–Alder formal catalizada por sales de oro. El proceso, que emplea amino ésteres propargílicos cuaternarios como sustratos de partida, conduce a la formación de una compleja estructura tetracíclica, con generación simultánea de cuatro enlaces y cinco estereocentros de manera altamente diastereoselectiva. Se han llevado a cabo cálculos teóricos que nos han permitido proponer un mecanismo que permite racionalizar el proceso tándem. Adicionalmente, mediante el estudio de la influencia de los ligandos en la reactividad de las reacciones catalizadas por oro, se han encontrado condiciones de reacción que permiten extender el proceso a amino ésteres de partida con una gran variedad de patrones de sustitución. Finalmente, la versión asimétrica del proceso tándem fue también objeto de estudio.*



R<sup>1</sup> = 4-MeO  
R<sup>2</sup> = Me, Et, Bn, CH<sub>2</sub>CH<sub>2</sub>TMS  
R<sup>3</sup> = CF<sub>3</sub>, CF<sub>2</sub>Cl, CF<sub>2</sub>CF<sub>2</sub>, allylCF<sub>2</sub>, Ph, Me, 4-Cl-C<sub>6</sub>H<sub>4</sub>, 4-MeO-C<sub>6</sub>H<sub>4</sub>, 2-naphthyl

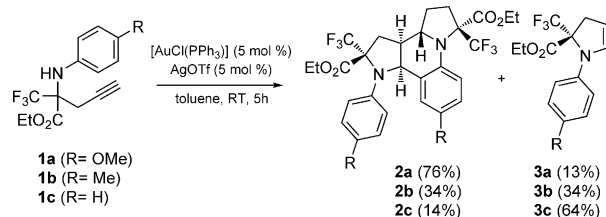
**Scheme 2.** Gold(I)-mediated tandem process with homopropargyl amino esters **1**.

curred, which gave rise to the final products as single diastereoisomers. Several fluorinated and non-fluorinated amino ester substrates **1** were compatible with this tandem protocol. Blocking the NH bond in the substrates (Scheme 1, R<sup>3</sup>, R<sup>4</sup> ≠ H) prevented the hydroamination step, and instead, a tandem hydroarylation/isomerization process occurred in the presence of gold salts to afford a new family of dihydroquinolines.<sup>[15]</sup>

The initial results of the tandem process (**via B**) showed that this reaction is very efficient when the aryl substituent is a PMP (*p*-methoxyphenyl) group; whereas, the use of other aromatic groups with different electronic properties led to a dramatic decrease in the product yields.<sup>[14]</sup> Herein, a careful investigation of the tandem process, mainly based on studying the effects of ligands on the gold catalyst, has allowed us to identify suitable conditions to extend the scope of this transformation to substrates with other types of aromatic substituents on the nitrogen atom. Theoretical studies have also been performed to shed light on the mechanism and the stereochemical outcome of the reaction. Additionally, the use of chiral substrates in this process is also discussed.

## Results and discussion

Initially, we sought to evaluate the differential reactivity of homopropargyl amines in the presence of gold salts based on the nature of the nitrogen protecting group. When fluorinated propargylic amino ester **1a** was treated with [AuCl(PPh<sub>3</sub>)] and AgOTf in toluene at room temperature, we observed the unexpected formation of tetracyclic compound **2a** in 76% yield together with a small amount (13% yield) of the hydroamination product **3a** (Scheme 3). Whilst studying the scope of this process, our attempts to extend the tandem protocol to include substrates that contained other N-aromatic substitution distinct from PMP were ineffective. With substrate **1b**, which bore a *p*-tolyl group, an equimolecular amount of **2b** and the hydroamination product **3b** were obtained; whereas, with sub-



**Scheme 3.** Gold(I)-mediated tandem protocol with amines **1a–c**.

strate **1c**, which contained a phenyl N-substituent, the hydroamination product **3c** was the major product.

To gain some insight into the mechanistic details of this transformation,<sup>[16]</sup> we carried out a theoretical study by using the density functional theory (DFT). In the gold(I)-mediated reactions described in this paper, [AuOTf(PPh<sub>3</sub>)] was assumed to be the catalytically active species and the complex [AuPMe<sub>3</sub>]<sup>+</sup> was used as a model in the theoretical study.<sup>[17]</sup> Full methodological details of this theoretical study are shown in the Supporting Information.

Based on the results of these calculations, we have proposed a plausible mechanistic explanation for the formation of the tetracyclic structures **2**; the proposed mechanism involves an initial hydroamination reaction of **1**, followed by an asymmetric dimerization pathway. The full process, which can be viewed as a formal aza-Diels–Alder reaction, is depicted in Scheme 4.

The initial step is the activation of the alkyne moiety of substrate **1a** through the coordination of the gold catalyst, which acts as a  $\pi$ -Lewis acid, with the triple bond. This step has a negligible energy barrier and proceeds to give complex **I**, which is 16.6 kcal mol<sup>-1</sup> more stable than the reactants. Cyclic intermediate **A** is then formed by the attack of the amine nitrogen atom on the triple bond in a favored 5-*endo*-dig cyclization.<sup>[18]</sup> Then, intermediate **A** releases a proton, which leads to the formation of triflic acid and intermediate **B**, which in turn reacts with triflic acid at the  $\beta$ -enaminic position to give two diastereoisomeric iminium salts **C<sub>syn</sub>** and **C<sub>anti</sub>**. The reaction of intermediates **C** with the triflate anion leads to the enaminic derivative **3a** and the catalyst [Au(L)OTf] is regenerated.<sup>[19]</sup>

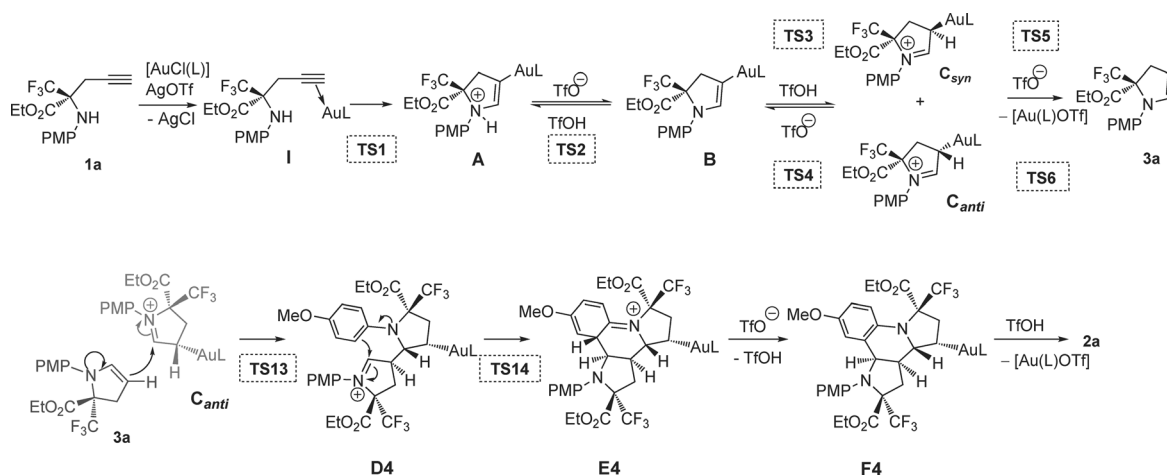
The most relevant geometrical and energetic features of the stationary points that were found for the transformation of compound **1a** into intermediates **C** and **3a** are shown in Figure 1. Complex **I** shows an asymmetric coordination of the AuPMe<sub>3</sub> moiety to the triple bond, and the C–C bond length is slightly increased (1.230 Å vs. 1.208 Å in **1a**). In this step, the alkyne moiety of substrate **1a** is activated by the gold catalyst; thus, the 5-*endo*-dig cyclization of complex **I** is favored. This

leads to intermediate **A**, which is a five-membered ring ammonium salt (Figure 1 a).

Transition state **TS1** shows one imaginary vibrational frequency with a normal mode that corresponds to the formation of the N–C bond, as expected for a hydroamination reaction. The distance between the two carbon atoms, which initially corresponds to a triple bond, increases from 1.208 Å in **1a** to 2.264 Å in **TS1**. Transition state **TS2**, involved in the deprotonation of intermediate **A**, shows an imaginary normal mode that corresponds to the proton transfer from the nitrogen atom of **A** to the oxygen atom of the triflate anion, which is a process that leads to the formation of intermediate **B**. As can be seen from the values of the N–H (1.420 Å) and O–H (1.129 Å) bond lengths in the transition state, the proton has already been transferred from the nitrogen atom of **A** to the oxygen atom of the triflate. The activation Gibbs free energy for each of these reactions was calculated to be 11.5 and 0.2 kcal mol<sup>-1</sup>, respectively (Figure 1 a).

The reaction at the  $\beta$ -position of the enaminic intermediate **B** with triflic acid, which gives rise to the diastereoisomeric iminium intermediates **C<sub>syn</sub>** and **C<sub>anti</sub>** was shown to take place through two possible transition states, **TS3** or **TS4**, depending on the stereochemistry of the proton addition (Figure 1 a). The imaginary normal mode in these transition states involves both the proton transfer and the shortening of the N–C bond. **TS3** presents an activation barrier of 2.3 kcal mol<sup>-1</sup> and gives rise to intermediate **C<sub>syn</sub>**; whereas, **TS4** is predicted to be 1.3 kcal mol<sup>-1</sup> less stable than **TS3**. Both intermediates, **C<sub>syn</sub>** and **C<sub>anti</sub>** show similar levels of stability; **C<sub>anti</sub>** is slightly energetically favored by 0.3 kcal mol<sup>-1</sup>.

The stationary points for the deauration reaction of intermediates **C<sub>syn</sub>** and **C<sub>anti</sub>** are shown in Figure 1 b. In these reactions, the hydroamination product **3a** is formed and the catalytically active species [AuOTf(PPh<sub>3</sub>)] is regenerated. The product **3a** can be formed from either **C<sub>syn</sub>** or **C<sub>anti</sub>** via the transition state structures **TS5** or **TS6**, respectively. The imaginary normal mode in these transition states corresponds to the formation of the bond between the gold and the oxygen atoms and the



**Scheme 4.** Mechanistic proposal for the gold-catalyzed transformation of amine **1a** into the tetracyclic structure **2a** (only the intermediates with the relative configuration that lead to the experimentally observed product **2a** are shown).

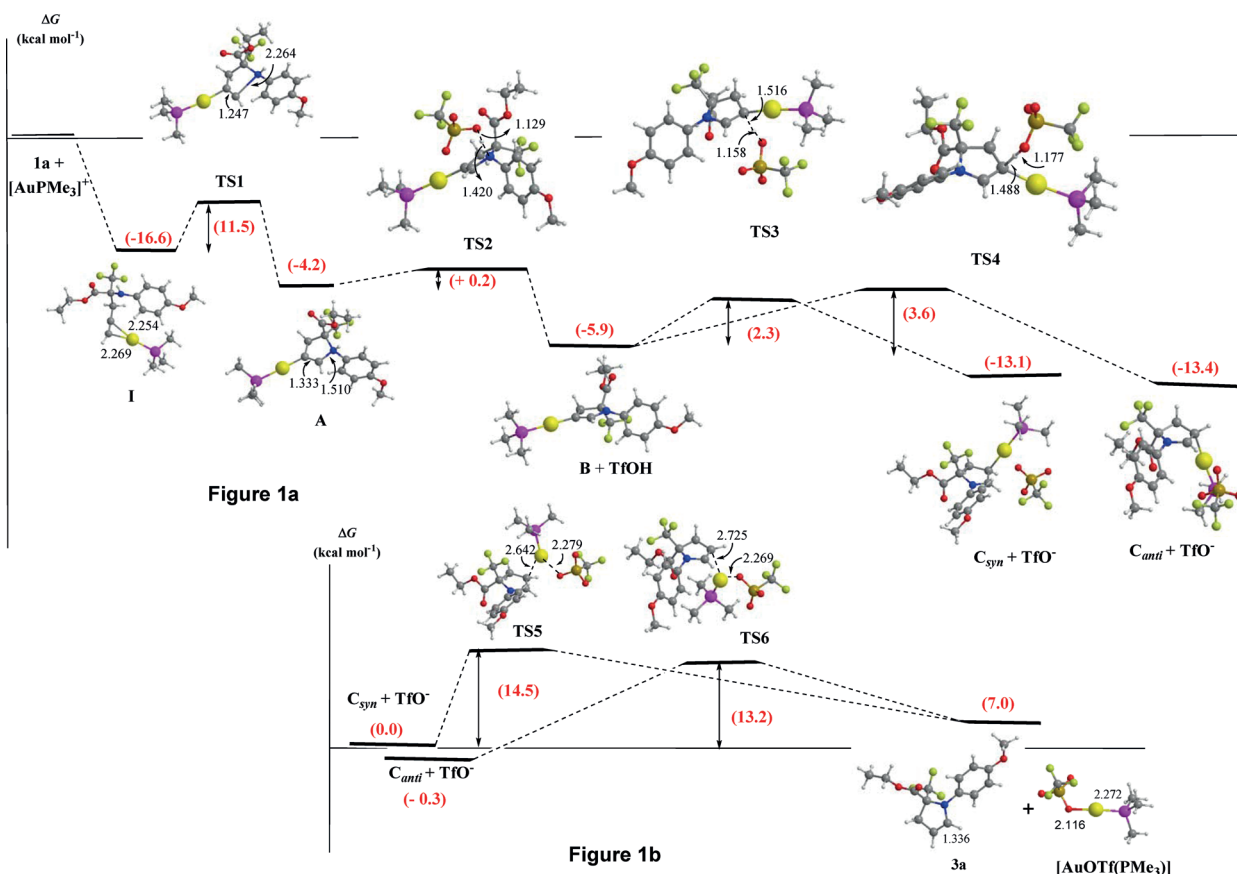


**Figure 1.** a) Stationary points located for the cyclization reaction of **1a**, which leads to intermediates  $C_{syn}$  and  $C_{anti}$ . b) Stationary points for the deauration reaction that leads to intermediate **3a** and the active catalytic species  $[AuOTf(PPh_3)]$  (bond lengths are in Å and Gibbs free energies in  $\text{kcal mol}^{-1}$ ).

breaking of the carbon–gold bond, as might be expected from nucleophilic attack of the triflate anion on the  $AuPMe_3$  moiety. The deaurations of both  $C_{syn}$  and  $C_{anti}$  are slightly endothermic and they have activation barriers of 14.5 and 13.2  $\text{kcal mol}^{-1}$ , respectively.

As shown in Scheme 4, an asymmetric dimerization pathway that involves **3a** and either  $C_{syn}$  or  $C_{anti}$  accounts for the formation of the tetracyclic skeleton of derivatives **2**. As both the nucleophilic carbon atom of **3a** and the electrophilic iminium carbon atom of **C** are prochiral (Figure 2), their addition reac-

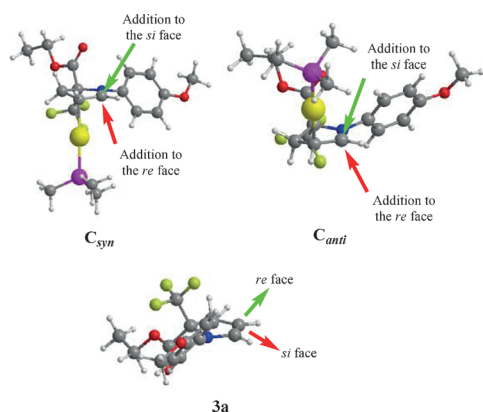


**Figure 2.** Relative stereochemistry of the addition reactions of **3a** with  $C_{syn}$  or  $C_{anti}$ .

tion could lead to the formation of eight diastereoisomers of intermediate **D**.

An intramolecular imine–iminium addition reaction via intermediates **D** leads to tetracyclic intermediates **E**. The TfO-promoted aromatization of **E** gives rise to intermediate **F** and triflic acid, which in turn will participate in the protodeauration of **F** to form the final product **2** (Scheme 4). According to the experimental evidence, the tetracyclic structures **2** are obtained in most cases as single diastereoisomers. This fact implies a high level of facial stereoselectivity in the addition of **3a** to iminium intermediate **C**.

The 32 stationary points located for each step of the transformation of **3a** into tetracyclic intermediate **E** are shown in the Supporting Information. The four reaction pathways with the lowest Gibbs free energies are presented in Figure 3. In the case of the reaction of **3a** with  $C_{anti}$  or  $C_{syn}$ , the lowest Gibbs free energies ( $\Delta G^\ddagger$ ) for the first step of the reaction are 27.6 (**TS17**), 28.2 (**TS7**), 29.6 (**TS9**), and 31.9  $\text{kcal mol}^{-1}$  (**TS13**). In the case of **TS17**, intermediate **D6** is not very stable and can easily revert back towards the reactants. The situation is even worse in the case of **D2**, which is only 0.4  $\text{kcal mol}^{-1}$  more stable than **TS9**. On the other hand, intermediate **D1** is 3.2  $\text{kcal mol}^{-1}$  more stable than **TS7**; however, the  $\Delta G^\ddagger$  for the cyclization step via **TS8** is very high. In the case of the reaction of **3a** with  $C_{anti}$  which possesses the relative *si/si* stereochemistry, intermediate **D4** is 6.8  $\text{kcal mol}^{-1}$  more stable than both **TS13** and **TS14**. In

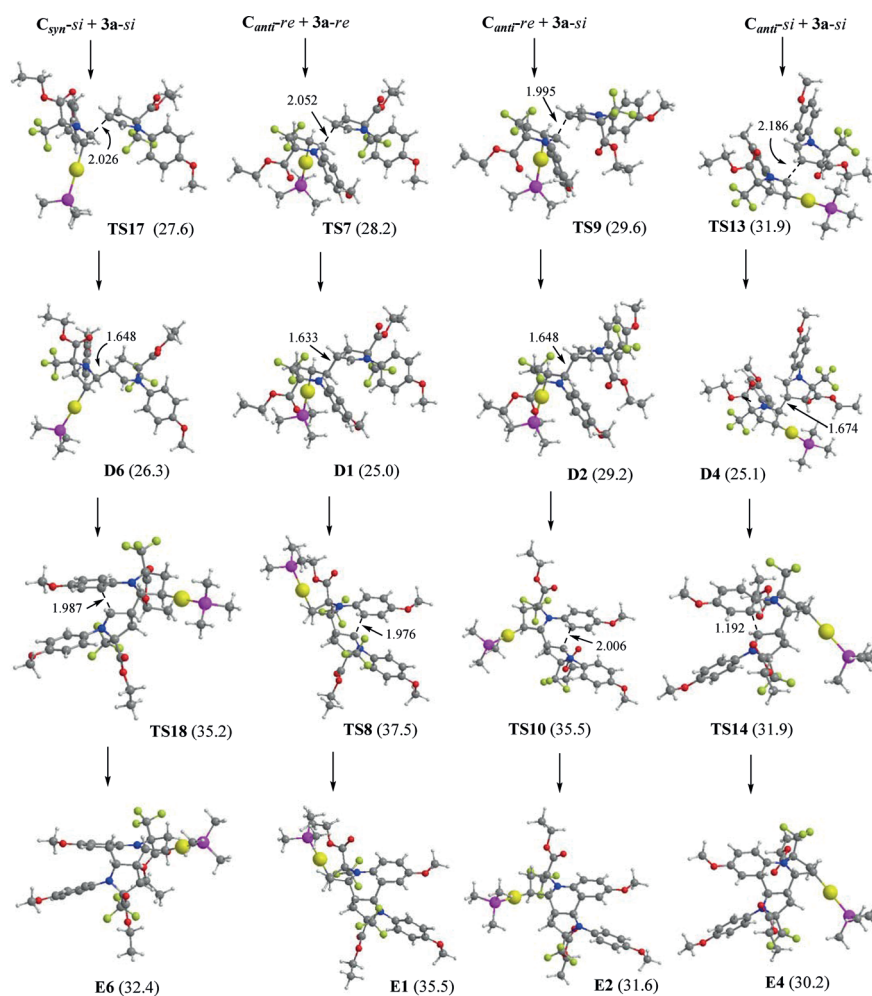


**Figure 3.** Stationary points located for the addition reaction of **3a** with intermediates  $C_{syn}$  and  $C_{anti}$ , with the specification of the reaction stereochemistry (bond lengths are in Å and Gibbs free energies in kcal mol<sup>-1</sup>).

this situation, the tetracyclic intermediate **E4** is expected to be formed preferentially and after the aromatization and deauration reactions it will give rise to final product **2a**.

As expected, the imaginary normal mode of **TS13** corresponds to the bond formation reaction between the iminium carbon atom of  $C_{anti}$  and the enaminic  $\beta$ -carbon atom of **3a**, which leads to intermediate **D4**. This intermediate contains two reactive centers: an electrophilic iminium carbon atom and an enamine-like fragment that is incorporated in the aromatic ring of the PMP group. Thus, **TS14**, as its imaginary normal mode shows, corresponds to the C–C bond formation that takes place between the aromatic *ortho*-carbon atom, relative to the nitrogen, and the iminium carbon atom. Overall, these last two steps may be considered together as a formal, stepwise aza-Diels–Alder reaction.

Owing to the high degree of functionalization of the reactants, it is not easy to single out just one factor that is responsible for the facial selectivity observed in this reaction. However, examination of the geometry of the transition state structures (**TS7**, **TS9**, **TS13**, and **TS17**) and the corresponding intermediates (**D1**, **D2**, **D4**, and **D6**) has shed some light on the origin of the observed stereochemical outcome. In the most

stable intermediates (Figure 4, **D1** and **D4**), the trifluoromethyl groups are in an *anti* relationship, relative to each other, which minimizes the steric interactions. This also ensures that the two aromatic rings are spatially close, such that two hydrogen atoms of the aromatic ring that corresponds to the **3a** moiety point towards the PMP ring. In addition, the steric effect of the trifluoromethyl group appears to strongly destabilise the transition state structure **TS18** relative to **TS14**, as shown in Figure 5 (see the Supporting Information). The combination of both of these steric interactions explains the selective formation of intermediate **E4** and the observed diastereoisomer of tetracyclic derivative **2a**.

Considering this reaction pathway, the key step for the success of the tandem process is the addition of the enaminic moiety of pyrroline **3** to the iminium functionality of  $C_{anti}$ . As the hydroamination product **3a** arises from the deauration of  $C_{anti}$ , a low rate of reaction is required in this step to increase the presence of intermediate

$C_{anti}$  and enable its reaction with **3a**.

As mentioned above, a recent study demonstrated that it is possible to categorize and tune-up most gold-catalyzed reactions through the careful choice of the ligand.<sup>[7]</sup> This study indicated that, when basic substrates were involved in the process, the protodeauration is the rate-determining step. The presence of strong acids in the reaction media that would increase the rate of protodeauration, such as triflic acid, is minimised by neutralisation with the basic substrate. In the present

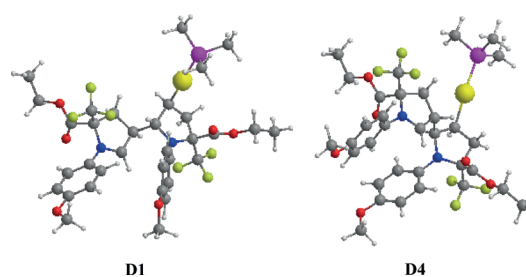


**Figure 4.** Geometry of intermediates **D1** and **D4**, showing the relative *anti* relationship of the CF<sub>3</sub> groups and the spatial proximity of the PMP rings.

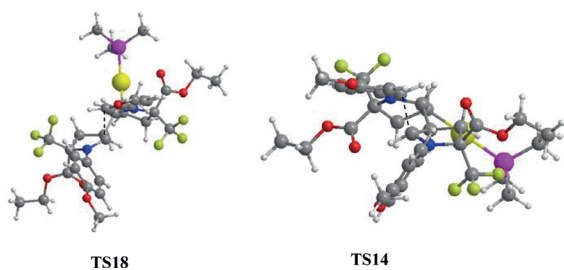


**Figure 5.** Geometry of transition state structures **TS18** and **TS14**, showing the relative position of the  $\text{CF}_3$  group.

case, the triflic acid, which is formed during the generation of the catalytic gold species, will be partially neutralised by the amine. This will decrease the rate of the deauration step and allow pyrroline **3a** to react with the iminium intermediate **C**.

With these considerations and on the basis of the proposed mechanism, it is possible to rationalise the different behavior of substrates **1a–c** (Scheme 3) in the tandem process. When the aromatic substituent at the nitrogen atom is the PMP group (**1a**), the electron-donating properties of the methoxy group increase the basicity of the nitrogen, which lowers the protodeauration rate, and this subsequently translated into an improved ability for the tandem reaction to proceed. With the *p*-tolyl and phenyl groups (**1b,c**), the basicity of the amine decreases, respectively, which increases the rate of deauration and in turn diminishes the formation of the tandem products.

According to the aforementioned studies of ligand effects on the kinetics of the deauration step,<sup>[7]</sup> an electron-rich ligand should accelerate this process. Conversely, electron-withdrawing ligands would decelerate the deauration step and, both in our case and based on the previous mechanistic discussion, they would favor the tandem transformation. To test this hypothesis, substrate **1c** was subjected to the tandem reaction conditions in the presence of gold salts that bore electronically deficient ligands relative to  $\text{PPh}_3$  (Table 1, entry 1).

The first attempt was performed with ligand **L1**, which contained three phenyl rings each with a 4-trifluoromethyl substituent. Initially, the reaction was performed in toluene at room temperature, with the gold salt generated in situ; we observed that, after 24 h, only 60% conversion was achieved. Nevertheless, the exclusive formation of tetracycles was detected, albeit as a mixture of diastereoisomers, in which the major compound was **2c**, which was isolated in 47% yield (entry 2). The use of  $\text{CH}_2\text{Cl}_2$  as the solvent led to an unexpected increase in the rate, with the reaction being completed in 1 h even at  $0^\circ\text{C}$ . In this case, the major isomer **2c** was isolated in 72% yield together with 3% yield of the hydroamination product **3c** (entry 3). Therefore, according to our hypothesis, ligand **L1** decreases the protodeauration rate, which favors the tandem process, albeit with some erosion of the selectivity, and minimizes the formation of the hydroamination product. Following the same reaction trend, the use of ligand **L2** in the tandem reaction provided tetracycle **2c** in 51% yield after 12 h in toluene, with complete conversion being observed in this case (entry 4). When  $\text{CH}_2\text{Cl}_2$  was used as the solvent and the reaction was performed at  $0^\circ\text{C}$ , **2c** was isolated in 55% yield

**Table 1.** Optimisation of the ligands in the tandem protocol.

The reaction scheme shows substrate **1c** reacting with  $[\text{Au}(\text{L})\text{Cl}]$  (5 mol %) and  $\text{AgOTf}$  (5 mol %) in a solvent at temperature  $T$  for time  $t$  to yield products **2c** and **3c**.

Chemical structures for ligands are shown below the reaction scheme:

- L1** ( $\text{R}=\text{CF}_3$ ): A phosphine ligand with three phenyl rings, each substituted with a trifluoromethyl group at the para position.
- L2** ( $\text{R}=\text{F}$ ): A phosphine ligand with three phenyl rings, each substituted with a fluorine atom at the para position.
- L3**: A phosphite ligand with three phenyl rings, each substituted with an isobutyl group at the para position.
- L4** (JackiePhos): A phosphine ligand with three phenyl rings, each substituted with a trifluoromethyl group at the para position, and a methoxy group at the ortho position.

Entry	Ligand	Solvent	$T$ [ $^\circ\text{C}$ ]	Time [h]	<b>3c</b> [%]	<b>2c</b> [%] <sup>[a]</sup>
1	$\text{PPh}_3$	toluene	25	5	64	14
2	<b>L1</b>	toluene	25	24	–	47 <sup>[b]</sup>
3	<b>L1</b>	$\text{CH}_2\text{Cl}_2$	0	1	3	72
4	<b>L2</b>	toluene	25	12	3	51
5	<b>L2</b>	$\text{CH}_2\text{Cl}_2$	0	2	3	55
6	<b>L3</b>	toluene	25	1	3	48
7	<b>L3</b>	$\text{CH}_2\text{Cl}_2$	0	2	1	51
8	<b>L3</b>	toluene	0	2	3	58
9	<b>L4</b>	toluene	25	24	3	55
10	<b>L4</b>	$\text{CH}_2\text{Cl}_2$	0	15	3	53

[a] Yield of the isolated major diastereoisomer. [b] 60% conversion.

(entry 5). When ligand **L3**, which contains the phosphite unit with the most electron-deficient substituents, was used in the tandem reaction, either in toluene or in  $\text{CH}_2\text{Cl}_2$ , the reaction was complete in 2 h; however, these conditions did not improve the reaction yield (entries 6–8). Finally, the use of JackiePhos **L4** afforded results that were comparable to the reaction with **L2** in terms of reaction time and yield of compound **2c**, in either toluene or  $\text{CH}_2\text{Cl}_2$  (entries 9 and 10).

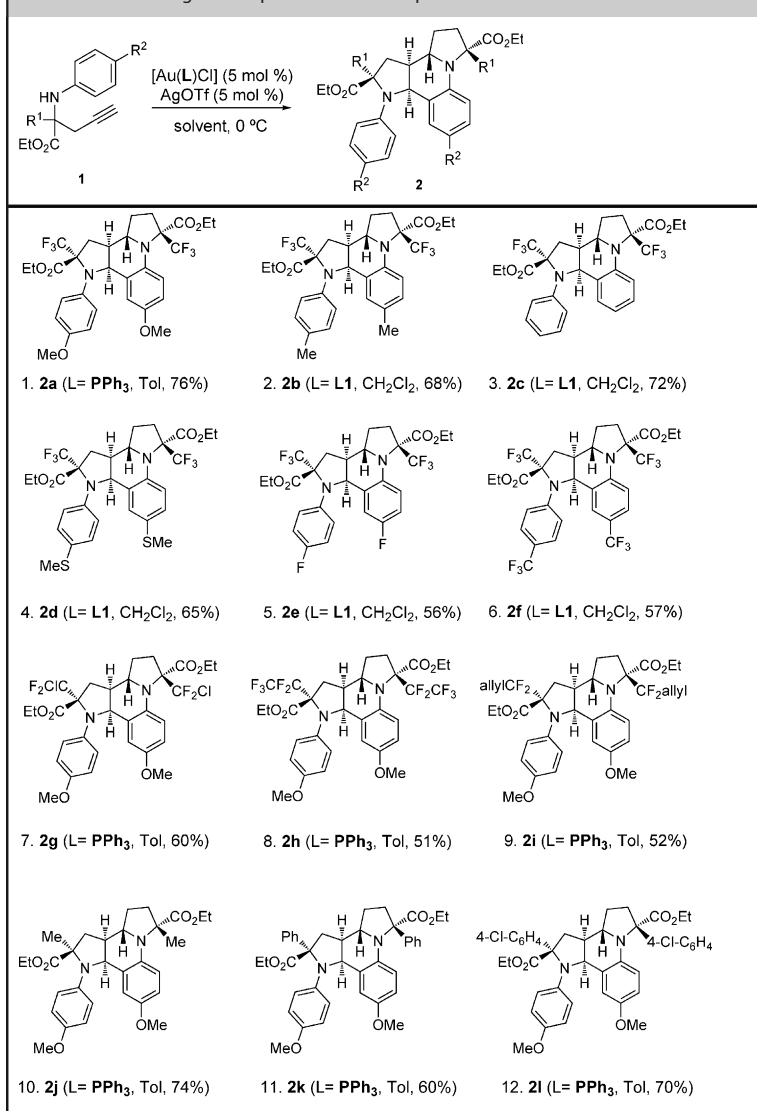
With these results in hand, we concluded that the optimum conditions to carry out the tandem process involve the use of ligand **L1** in  $\text{CH}_2\text{Cl}_2$  at  $0^\circ\text{C}$ , when the amino ester substrates contain electron-poor aromatic N-substituents. These conditions were applied to other amine substrates **1** and the results that were obtained are summarised in Table 2.

Substrates **1b–f**, which bear a variety of electron-donating and electron-withdrawing substituents on the aromatic ring (other than PMP), underwent the tandem protocol very efficiently to afford tetracycles **2b–f** in good yields (Table 2, entries 2–6). Substrates with fluorinated (entries 1, 7–9) and non-fluorinated (aliphatic: entry 10, aromatic: entries 11 and 12) substituents at the alpha position relative to the nitrogen atom were also compatible with the process, when  $\text{PPh}_3$  was used as the ligand (when  $\text{R}^2=\text{OMe}$ ).

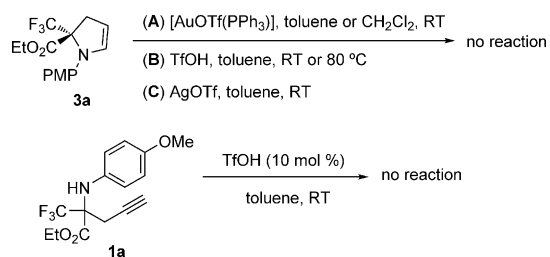
In summary, the results from the experimental ligand study and the theoretical calculations led us to identify suitable conditions to broaden the scope of our tandem protocol, just by changing the ligand of the gold(I) salt and the solvent. Notably, all of the final products contain two alpha amino acid units.

Additional experiments were performed to provide further evidence for the mechanistic pathway that was proposed

**Table 2.** Broadening the scope of the tandem protocol.



above. It is important to mention that the cyclization step would be further promoted by either the triflic acid or the gold salt. Accordingly, several authors have suggested that hydroamination products analogous to **3a–c** could be protonated by triflic acid, which would give rise to iminium intermediates of type **C**, thus initiating a dimerization protocol.<sup>[20]</sup> It is also known that gold salts can activate enamines and enol ethers for the nucleophilic attack.<sup>[21]</sup> To prove our mechanistic

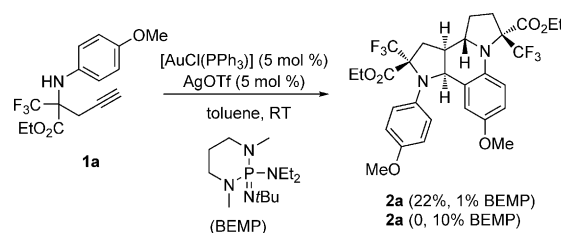


**Scheme 5.** Reactivity evaluation of **1a** and **3a**.

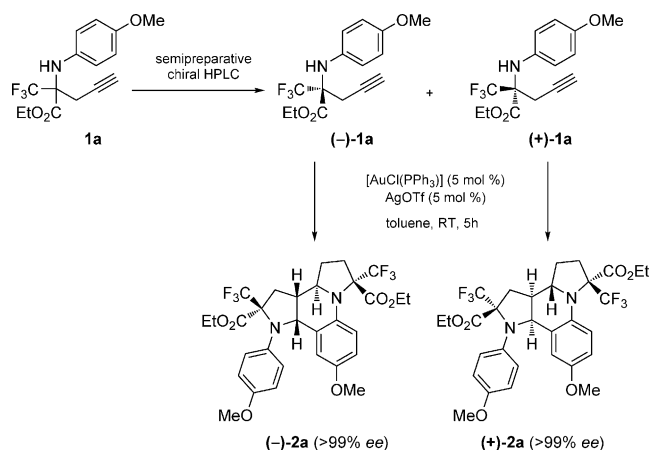
proposal, substrate **3a** was independently treated with [AuOTf(PPh<sub>3</sub>)] (Scheme 5, conditions **A**), triflic acid (conditions **B**), and the silver salt (conditions **C**). In all cases, the starting material remained unaltered, even when the reaction was heated at 80 °C for several hours. Alternatively, hydroamination reactions can also be promoted by Brønsted acids;<sup>[22]</sup> therefore, triflic acid could be the catalyst of the tandem protocol. However, no reaction was observed when compound **1a** was treated with triflic acid in toluene after 24 h at RT (Scheme 5); therefore, triflic acid is not the catalyst of the process. These observations are also in agreement with the relevance of intermediate **C** (Scheme 4) in our tandem process and they corroborate the fact that the hydroamination product, by itself, does not undergo the tandem protocol.

In addition, compound **1a** was subjected to the gold-catalyzed reaction conditions in the presence of BEMP (2-tert-butylimino-2-diethylamino-1,3-dimethylperhydro-1,3,2-diazaphosphorine), a non-poisoning base. In the presence of 10 mol% BEMP and 5 mol% of the gold catalyst, the reaction did not proceed and the starting material was recovered unaltered (Scheme 6). With 1 mol% BEMP and 5 mol% of the gold catalyst, the rate of reaction was slowed, and after 20 h at RT only 22% conversion was reached (Scheme 6). The former experiment, with 10 mol% BEMP, indicates that all the triflic acid that is necessary to close the gold catalytic cycle is captured by the base, which inhibits the tandem process. However, with 1 mol% BEMP the tandem process is diminished but not eliminated. Therefore, the gold species can act as a Brønsted acid to catalyze the formal azadiels–Alder reaction; consequently, this alternative mechanism for the tetracycle formation cannot be overruled.<sup>[23]</sup>

The last step of our study was the development of an asymmetric version of the tandem protocol. Accordingly, substrate **1a** was subjected to chiral HPLC and, once conditions to separate the enantiomers in a semi-preparative manner were identified, we isolated both enantiomers separately.<sup>[24]</sup> Each enantiomer was independently treated with [Au(OTf)PPh<sub>3</sub>] in toluene at room temperature, and clean formation of the corresponding tetracycles **2a** as single enantiomers was observed by analytical chiral HPLC (Scheme 7).



**Scheme 6.** Gold-catalyzed process in the presence of BEMP.



Scheme 7. The asymmetric tandem protocol.

## Conclusion

A tandem hydroamination/formal aza-Diels–Alder reaction of homopropargyl amino esters **1** is described, which gives rise to tetracyclic structures **2** in good yields and stereoselectivities. Theoretical calculations led us to propose all the intermediates of the process and to rationalise the formation of the final products as well as the stereochemical outcome of the reaction. In combination with a ligand screening, these studies permitted us to broaden the reaction scope to include substrates that contained substituted aromatic rings with diverse electronic properties. Notably, the use of enantiomerically pure starting materials indicated that the process is stereospecific.

## Acknowledgements

We would like to thank the Spanish Ministerio de Economía y Competitividad (CTQ-2013-43310-P) and Generalitat Valenciana (GV/PrometeoII/2014/073) for their financial support. J.M. would like to thank University of Valencia for a predoctoral fellowship.

**Keywords:** aza-Diels–Alder · density functional calculations · gold · hydroamination · tandem reaction

- [1] For recent reviews on hydroamination reactions, see: a) H. Hannedouche, E. Schulz, *Chem. Eur. J.* **2013**, *19*, 4972; b) T. E. Müller, K. C. Hultzsich, M. Yus, F. Foubelo, M. Tada, *Chem. Rev.* **2008**, *108*, 3795; c) R. Severin, S. Doye, *Chem. Soc. Rev.* **2007**, *36*, 1407; d) R. A. Widenhofer, X. Han, *Eur. J. Org. Chem.* **2006**, 4555.
- [2] See, for example: a) H. Ohno, H. Chiba, S. Inuki, S. Oishi, N. Fujii, *Synlett* **2014**, 179; b) N. T. Patil, V. Singh, *J. Organomet. Chem.* **2011**, *696*, 419.
- [3] a) A. S. K. Hashmi, M. Bührle, *Aldrichimica Acta* **2010**, *43*, 27; b) M. Rudolph, A. S. K. Hashmi, *Chem. Commun.* **2011**, *47*, 6536; c) D.-H. Zhang, Z. Zhang, M. Shi, *Chem. Commun.* **2012**, *48*, 10271; d) N. Krause, C. Winter, *Chem. Rev.* **2011**, *111*, 1994; e) H. C. Shen, *Tetrahedron* **2008**, *64*, 3885; f) H. C. Shen, *Tetrahedron* **2008**, *64*, 7847.
- [4] a) D.-H. Zhang, X.-Y. Tang, M. Shi, *Acc. Chem. Res.* **2014**, *47*, 913; b) H. Ohno, *Isr. J. Chem.* **2013**, *53*, 869; c) Y.-P. He, H. Wu, D.-F. Chen, J. Yu, L.-Z. Gong, *Chem. Eur. J.* **2013**, *19*, 5232; d) A. S. K. Hashmi, M. Bührle, M. Wölflle, M. Rudolph, M. Wieteck, F. Rominger, W. Frey, *Chem. Eur. J.* **2010**, *16*, 9846.

- [5] A. S. K. Hashmi, A. M. Schuster, F. Rominger, *Angew. Chem. Int. Ed.* **2009**, *48*, 8247; *Angew. Chem.* **2009**, *121*, 8396.
- [6] a) C. M. Krauter, A. S. K. Hashmi, M. Pernpointner, *ChemCatChem* **2010**, *2*, 1226; b) A. S. K. Hashmi, *Catal. Today* **2007**, *122*, 211.
- [7] W. Wang, G. B. Hammond, B. Xu, *J. Am. Chem. Soc.* **2012**, *134*, 5697.
- [8] D. J. Gorin, B. D. Sherry, F. D. Toste, *Chem. Rev.* **2008**, *108*, 3351.
- [9] For recent representative examples, see: a) Z. Zheng, H. Tu, L. Zhang, *Chem. Eur. J.* **2014**, *20*, 2445; b) C. Shu, L. Li, Y.-F. Yu, S. Jiang, L.-W. Ye, *Chem. Commun.* **2014**, *50*, 2522; c) Y.-F. Yu, C. Shu, C.-H. Shen, T.-Y. Li, L.-W. Ye, *Chem. Asian J.* **2013**, *8*, 2920; d) C. Shu, M.-Q. Liu, S.-S. Wang, L. Li, L.-W. Ye, *J. Org. Chem.* **2013**, *78*, 3292; e) L. Liu, L. Zhang, *Angew. Chem. Int. Ed.* **2012**, *51*, 7301; *Angew. Chem.* **2012**, *124*, 7413; f) H. Kim, Y. H. Rhee, *J. Am. Chem. Soc.* **2012**, *134*, 4011; g) H.-S. Yeom, E. So, S. Shin, *Chem. Eur. J.* **2011**, *17*, 1764; h) L. Cui, C. Li, L. Zhang, *Angew. Chem. Int. Ed.* **2010**, *49*, 9178; *Angew. Chem.* **2010**, *122*, 9364; i) C. Kim, H. J. Bae, J. H. Lee, W. Jeong, H. Kim, V. Sampath, Y. H. Rhee, *J. Am. Chem. Soc.* **2009**, *131*, 14660.
- [10] For analogous type of reactivity, see: a) J. P. Weyrauch, A. S. K. Hashmi, A. Schuster, T. Hengst, S. Schetter, A. Littmann, M. Rudolph, M. Hamzic, J. Visus, F. Rominger, W. Frey, J. W. Bats, *Chem. Eur. J.* **2010**, *16*, 956; b) A. S. K. Hashmi, J. P. Weyrauch, W. Frey, J. W. Wats, *Org. Lett.* **2004**, *6*, 4391.
- [11] For analogous type of reactivity, see: a) G. Cera, S. Piscitelli, M. Chiarucci, G. Fabrizi, A. Goggiamani, R. S. Ramón, S. P. Nolan, M. Bandini, *Angew. Chem. Int. Ed.* **2012**, *51*, 9891; *Angew. Chem.* **2012**, *124*, 10029; b) D. D. Vachhani, V. P. Mehta, S. G. Modha, K. Van Hecke, L. Van Meervelt, E. V. Van der Eycken, *Adv. Synth. Catal.* **2012**, *354*, 1593; c) Y. Zhang, J. Zhang, *Adv. Synth. Catal.* **2012**, *354*, 2556; d) M. Zhang, J. Zhang, *Chem. Commun.* **2012**, *48*, 6399.
- [12] For analogous type of reactivity, see: M. Zhu, W. Fu, G. Zou, C. Xun, D. Deng, B. Ji, *J. Fluorine Chem.* **2012**, *135*, 195.
- [13] S. Fustero, J. Miró, M. Sánchez-Roselló, C. del Pozo, *Chem. Eur. J.* **2014**, *20*, 14126.
- [14] S. Fustero, P. Bello, J. Miró, M. Sánchez-Roselló, M. A. Maestro, J. González, C. del Pozo, *Chem. Commun.* **2013**, *49*, 1336.
- [15] M. Sánchez-Roselló, J. Miró, C. del Pozo, S. Fustero, *J. Fluorine Chem.* **2014**, ahead of print, doi.org/10.1016/j.jfluchem.2014.09.017.
- [16] A. S. K. Hashmi, *Angew. Chem. Int. Ed.* **2010**, *49*, 5232; *Angew. Chem.* **2010**, *122*, 5360.
- [17] For a theoretical study on the nature of the catalytically active species in gold(I)-mediated reactions, see G. Kovács, G. Ujaque, A. Lledós, *J. Am. Chem. Soc.* **2008**, *130*, 853.
- [18] For a recent review on Baldwin's rules in alkyne cyclization reactions, see: K. Gilmore, I. V. Alabugin, *Chem. Rev.* **2011**, *111*, 6513.
- [19] A situation in which a triflate anion participates in a protodeauration reaction is described in reference [11].
- [20] a) A. Galván, J. Calleja, F. J. Fañanas, F. Rodríguez, *Angew. Chem. Int. Ed.* **2013**, *52*, 6038; *Angew. Chem.* **2013**, *125*, 6154; b) see reference [9c].
- [21] For some representative examples, see: a) K. Goutham, N. S. V. M. Rao Mangina, S. Suresh, P. Raghavaiah, G. V. Karunakar, *Org. Biomol. Chem.* **2014**, *12*, 2869; b) M. Chiarucci, M. di Lillo, A. Romaniello, P. G. Cozzi, G. Cera, M. Bandini, *Chem. Sci.* **2012**, *3*, 2859; c) J. A. Kozak, B. O. Patrick, G. R. Dake, *J. Org. Chem.* **2010**, *75*, 8585; d) A. Saito, T. Yang, A. Ferrali, L. Campbell, D. J. Dixon, *Chem. Commun.* **2008**, 2923; e) J. H. Teles, S. Brode, M. Chabanas, *Angew. Chem. Int. Ed.* **1998**, *37*, 1415; *Angew. Chem.* **1998**, *110*, 1475.
- [22] a) Z. Li, J. Zhang, C. Brouver, C.-G. Yang, N. W. Reich, C. He, *Org. Lett.* **2006**, *8*, 4175; b) D. C. Rosenfeld, S. Shekhar, A. Takemiya, M. Utsunomiya, J. F. Hartwig, *Org. Lett.* **2006**, *8*, 4179; c) J. Zhang, C.-G. Yang, C. He, *J. Am. Chem. Soc.* **2006**, *128*, 1798; d) K. Miura, A. Hosomi, *Synlett* **2003**, 143.
- [23] The behavior of gold salts as Brønsted acids has been previously invoked in gold-catalyzed processes: T. Yang, L. Campbell, D. J. Dixon, *J. Am. Chem. Soc.* **2007**, *129*, 12070, and references cited therein.
- [24] For the determination of the absolute configuration of enantiomerically pure substrates **1a**, see the Supporting Information.

Received: November 25, 2014

Published online on February 20, 2015